Clim Dyn (2012) 38:897–911
DOI 10.1007/s00382-011-1052-y

Dependence of climate forcing and response on the altitude of black carbon aerosols

George A. Ban-Weiss · Long Cao · G. Bala · Ken Caldeira

Received: 25 August 2010 / Accepted: 18 March 2011 / Published online: 9 April 2011

Abstract Black carbon aerosols absorb solar radiation and decrease planetary albedo, and thus can contribute to climate warming. In this paper, the dependence of equilibrium climate response on the altitude of black carbon is explored using an atmospheric general circulation model coupled to a mixed layer ocean model. The simulations model aerosol direct and semi-direct effects, but not indirect effects. Aerosol concentrations are prescribed and not interactive. It is shown that climate response of black carbon is highly dependent on the altitude of the aerosol. As the altitude of black carbon increases, surface temperatures decrease; black carbon near the surface causes surface warming, whereas black carbon near the tropopause and in the stratosphere causes surface cooling. This cooling occurs despite increasing planetary absorption of sunlight (i.e. decreasing planetary albedo). We find that the trend in surface air temperature response versus the altitude of black carbon is consistent with our calculations of radiative forcing after the troposphere, stratosphere, and land surface have undergone rapid adjustment, calculated as "regressed" radiative forcing. The variation in climate response from black carbon at different altitudes occurs largely from different fast climate responses; temperature dependent feedbacks are not statistically distinguishable. Impacts of black carbon at various altitudes on the hydrological cycle are also discussed; black carbon in the lowest atmospheric layer increases precipitation despite reductions in solar radiation reaching the surface, whereas black carbon at higher altitudes decreases precipitation.

Keywords Black carbon · Aerosol · Soot · Climate change · Global warming · Altitude · Fast response · Climate sensitivity · Feedback parameter

1 Introduction

Atmospheric aerosols alter Earth's energy balance by scattering and absorbing solar radiation (Seinfeld and Pandis 1998). The effect of aerosols on longwave and shortwave radiation at the top of the atmosphere depends on the relative amount of scattering and absorbing they perform; any combination of scattering and/or absorbing (the sum of which is extinction) leads to a reduction of downward solar radiation at the surface. Non-absorbing aerosols, such as sulfates, reflect incoming solar radiation and thus cool the Earth surface. In contrast, absorbing aerosols including black carbon absorb solar radiation and thus can warm the planet. Black carbon aerosols are now believed to be among the most important anthropogenic global warming agents (IPCC 2007; Ramanathan and Carmichael 2008).

Radiative forcing is a concept that has been introduced as a convenient way to compare climate change from different forcing agents under the assumption that radiative forcing is a good predictor of surface temperature response (IPCC 1990). There are different definitions and methods of calculating radiative forcing (Hansen et al. 1997) that

Electronic supplementary material The online version of this article (doi:10.1007/s00382-011-1052-y) contains supplementary material, which is available to authorized users.

G. A. Ban-Weiss (✉) · L. Cao · K. Caldeira
Department of Global Ecology, Carnegie Institution, 260 Panama Street, Stanford, CA 94305, USA
e-mail: georgebw@stanford.edu; georgebw@berkeley.edu

G. Bala
Divecha Center for Climate Change and Center for Atmospheric and Ocean Sciences, Indian Institute of Science, Bangalore 560012, India

have been proposed to maximize the predictability and comparability of equilibrium climate response by different forcing agents. These different methods calculate change in planetary energy balance at different atmospheric levels (i.e. usually either at the tropopause, top of the atmosphere, or surface) and at different times. The most commonly used definitions of radiative forcing (Hansen et al. 1997, 2005) aim to calculate planetary energy balance (1) immediately after introducing the forcing agent, usually termed "instantaneous radiative forcing," (2) after the stratosphere has adjusted to the forcing agent (on the order of months), termed "adjusted radiative forcing," or (3) after the troposphere, stratosphere, and land surface has undergone "rapid adjustment" to the forcing agent. The aforementioned rapid adjustment includes "fast responses" of the climate system that occur before significant changes in global- and annual-mean surface temperature (Gregory et al. 2004; Bala et al. 2009). The two most common ways of calculating radiative forcing after rapid adjustment of the climate system are to (1) quantify the difference in top of atmosphere radiative imbalance between two multi-year simulations (one with the imposed forcing agent and one without) with fixed sea surface temperatures, often termed either "fixed-SST forcing" (e.g. Hansen et al. 1997) or "radiative flux perturbation" (e.g. Haywood et al. 2009; Lohmann et al. 2010), and (2) determine the *y*-intercept of a linear regression of global annual averages of radiative imbalance at the top of atmosphere versus change in surface temperature, first presented by Gregory et al. (2004). To our knowledge this second approach has never been given a definitive name other than "forcing", so we refer to it in this paper as "regressed radiative forcing." Note that a potentially better approach than (1) is to fix both sea surface and land surface temperatures (Shine et al. 2003), though this is more difficult in practice. (There is no unique partitioning of changes of Earth's radiation budget into "forcings" and "feedbacks"; the most sensible partitioning depends on the goals of the specific analysis. Depending on the purpose of the study, it may make more sense to treat, for example, responses of the land biosphere as part of the forcing or part of the feedback.)

Absorbing aerosols are amongst the most challenging of forcing agents to determine a suitable definition of radiative forcing for accurately predicting climate response. Instantaneous and adjusted forcing have been shown to be ineffective at predicting climate response in part because of the significant cloud responses that these aerosols can cause on fast time-scales (Hansen et al. 1997, 2005; Cook and Highwood 2004). Both fixed-SST and regressed radiative forcing include fast cloud responses (as well as changes in temperature and water vapor profiles, and land surface temperatures) and thus have been shown to more accurately predict climate response (Hansen et al. 2005). The downfall of including atmospheric fast climate responses in the calculation of radiative forcing is that additional intermodel variation will be introduced, and thus a metric that is desired to be largely model independent becomes increasingly model dependent. By their very nature, all methods of computing radiative forcing except for the instantaneous forcing include some components of climate response in the definition of forcing. In the case of adjusted forcing, intermodel differences in stratospheric adjustment are likely to be small; however, fixed-SST and regressed radiative forcing depend in part on cloud responses, and thus significant intermodel differences may occur.

The climate effects of black carbon aerosols depend on their altitude in the atmosphere (Hansen et al. 1997, 2005; Haywood and Ramaswamy 1998; Ramanathan et al. 2001b; Seinfeld 2008). One of the first indications that this may be the case came from modeling studies from the 1980s simulating the climate impact of a hypothetical nuclear war (e.g. Turco et al. 1983; Covey et al. 1984; Cess 1985; Ramaswamy and Kiehl 1985). Though black carbon is generally thought of as a global warming agent, these studies suggested that large concentrations of absorbing aerosols in the upper troposphere and stratosphere would lead to surface temperature decreases. Hansen et al. (1997) used the Wonderland model, which is an idealized general circulation model (GCM) with idealized geography covering 120° of longitude, to show that the vertical distribution of tropospheric absorbing aerosols is likely to affect surface temperatures. This was shown using idealized simulations that altered the optical depth of various atmospheric layers in their model. Another study (Cook and Highwood 2004) using the Reading Intermediate General Circulation Model (IGCM) altered the optical depths and single scattering albedos of the lower and mid-troposphere separately to show the importance of cloud changes from absorbing aerosols; cloud response was shown to be different for absorbing aerosols in the lower troposphere versus mid troposphere. A study by Penner et al. (2003) using an enhanced version of the CRANTOUR/CCM GCM with fixed sea surface temperatures and prescribed aerosol emissions, and thus predicted aerosol concentrations, showed that emitting a mixture of black and organic carbon, referred to collectively as "soot", at a high altitude could cause negative fixed-SST radiative forcing (which they refer to as "relaxed" forcing). Hansen et al. (2005) used the GISS Model E GCM to investigate the "efficacy" of various climate forcing agents, where efficacy was defined as the global temperature response per unit forcing for a given agent relative to that response to CO_2 forcing. One of the many forcing agents investigated was black carbon aerosols at different layers in the troposphere. It was found that instantaneous, adjusted, and fixed-

SST radiative forcing, and changes in surface temperature, were dependent on the altitude of black carbon in the troposphere. A comparison to Penner et al. and Hansen et al. (2005) can be found in the Sect. 4.

We build on the previous work by investigating the dependence of regressed radiative forcing and equilibrium climate response on the altitude of black carbon aerosols using an atmospheric general circulation model with a mixed layer ocean model. This was carried out using the NCAR Community Atmosphere Model (CAM3.1) (Collins et al. 2004) by performing six idealized simulations, each of which added 1 Mt (10^6 ton) of black carbon aerosol uniformly around the globe to a different horizontal model layer in the atmosphere, ranging from the surface layer to layers in the stratosphere. Aerosols were prescribed and not interactive. We start by discussing regressed radiative forcing and the fast response of the climate system using the regression method of Gregory et al. (2004); here fast response refers to changes in the atmosphere that occur before longer time-scale changes in global and annual-average temperature (Bala et al. 2009). A comparison of regressed radiative forcing to fixed-SST radiative forcing is made using the results of additional simulations with fixed-SSTs. We then present results of climate response after the climate reaches equilibrium. Hansen et al. (2005) presented results of various measures of radiative forcing and surface temperature change from black carbon aerosols in various layers in the troposphere. We build on this study by investigating additional altitudes higher in the troposphere and in the stratosphere, and include an analysis of the hydrological cycle, surface energy balance, and cloud response; we also use a different GCM.

2 Methods

2.1 Simulations

In this study, each simulation added 1 Mt (10^6 ton) of black carbon aerosol uniformly around the globe to a different horizontal layer in the atmosphere, ranging from the surface layer to layers in the stratosphere. This added black carbon was additional to modern background aerosol concentrations (further discussed in the Sect. 2.4). We used a configuration of the CAM3.1 model that represents the atmosphere with 26 layers in a sigma hybrid vertical coordinate system. We added black carbon to layers 0 (bottom layer), 3, 6, 13, 20, and 23 (two layers below the top layer), corresponding approximately to altitudes of 0 km (near-surface), 1, 4, 12, 20, and 29 km, respectively. (The latter two layers are in the stratosphere, and 12 km is in the upper troposphere at low latitudes and in the lower stratosphere at high latitudes.) We refer to each simulation using these nominal altitudes. We also reference the 12 km simulation as being near the tropopause. To facilitate attribution of changes in climate to black carbon at various altitudes, careful control of aerosol altitude is important; thus, we prescribe time-invariant concentrations for *additional* black carbon in each simulation, rather than prescribing aerosol emissions. Our approach was similar to that of Hansen et al. (2005), but different than that of Penner et al. (2003) who investigated the effect of increasing aerosol emissions at an elevated altitude. Our simulations are idealized and are intended to elucidate fundamental properties of the climate system; this study is not intended to realistically represent current or future atmospheric aerosol distributions. Our analysis includes direct effects (i.e., radiation scattering and absorption by aerosols) and semi-direct effects (i.e., changes in climate due to the local heating from black carbon). Indirect aerosol effects, in which particles act as cloud condensation nuclei, are not considered here. We also do not include the direct impact of black carbon on surface albedo (i.e. deposition of aerosols on the Earth surface).

2.2 Calculation of regressed radiative forcing, fixed-SST radiative forcing, fast climate response, and equilibrium climate response

In this study we calculate regressed radiative forcing, fast response of clouds, and equilibrium climate response. We calculate regressed radiative forcing and the fast response of clouds using the regression method of Gregory et al. (2004), taking the y-intercept of regressions of the variables of interest versus changes in surface air temperature. Regressed radiative forcing uses this regression method with the net radiative fluxes at the top of the atmosphere. Annual means of the first 20 years of the simulations are used in the regressions. To decrease uncertainty in the regressions, we ran two additional 20-year simulations for each case of increased black carbon, and thus for each case the regressions were based on annual averages of the ensemble mean. The equilibrium climate response is calculated by averaging the climatically relevant variables after a steady state is approached. The model approaches a steady state within 30 years, and results for the last 70 years of each 100-year simulation are presented. The slow climate response can be calculated as the slope of the regressions (Gregory et al. 2004) or as the equilibrium response minus the fast response (Bala et al. 2009). We also performed additional simulations using prescribed climatological SSTs to facilitate a comparison of regressed radiative forcing to fixed-SST radiative forcing. Results presented for the fixed-SST radiative forcing are averages of the last 35 years of 40-year simulations.

2.3 Model details

The CAM3.1 model used in this study has 2 × 2.5° (longitude × latitude) resolution, and is coupled to the Community Land Model (CLM3.0) (Oleson et al. 2004) with a slab-ocean/thermodynamic sea ice model. Each simulation was run with a prescribed CO_2 concentration of 780 ppm. Results for each simulation are presented relative to results from a control simulation with this same CO_2 concentration and modern background aerosol concentrations, discussed further in the next section.

2.4 Aerosols in CAM3.1

The CAM3.1 model represents five different aerosol types: sea salt, soil dust (four different sizes), black and organic carbon, and sulfate (Collins et al. 2004). An aerosol assimilation system is used to produce present-day three-dimensional monthly aerosol distributions of aerosol mass (Collins et al. 2001, 2002). This system consists of an assimilation of satellite retrievals of aerosol optical depth from the NOAA Pathfinder II data set (Stowe et al. 1997), and the Model for Atmospheric Chemistry and Transport (MATCH) (Rasch et al. 1997), which uses the National Centers for Environmental Prediction (NCEP) reanalysis data (Kalnay et al. 1996). Each of our simulations added 1 Mt of black carbon to a different horizontal layer in the atmosphere on top of these present-day aerosol distributions. For reference, annual emissions of black carbon have been estimated to be ~8 Mt year^{-1} (Bond et al. 2004). Thus, our addition of 1 Mt black carbon in each simulation is on the order of 10% annual emissions, but several times larger than the average global atmospheric loading of ~0.2 Mt found in the present day aerosol dataset used. We use this large loading to ensure that our results are statistically different than the control simulation.

CAM3.1 uses three intrinsic optical properties for each aerosol type: specific extinction, single scattering albedo, and asymmetry parameter (Collins et al. 2004). For carbonaceous aerosols, these optical properties come from the optical properties of aerosols and clouds (OPAC) data set (Hess et al. 1998). The optical properties for black carbon in this study are identical to "soot" in OPAC and are dependent on wavelength. CAM3.1 interpolates the wavelength dependent optical properties from OPAC onto a 20 cm^{-1} uniform wavenumber grid ranging from 49,980 to 260 cm^{-1}, and then averages them onto the 19-band shortwave spectrum used in CAM3.1. For black carbon, the single scattering albedo ranges from 0.004 to 0.314 (dimensionless), the specific extinction ranges from 0.88 to 23.5 m g^{-1}, and the asymmetry parameter ranges from 0.05 to 0.53 (dimensionless), depending on wavelength. Black carbon is assumed not to absorb longwave radiation.

3 Results

Here, we analyze first the radiative forcing imposed by black carbon addition in various model layers, and then analyze the climate response to those radiative forcings.

3.1 Regressed radiative forcing and fast response of clouds

Regressed radiative forcing and the fast response of cloud variables is shown in Table 1 (see Figure S1 in Online Resource 1 for the regressions). Addition of 1 Mt of black carbon to the lowest atmospheric layer (~0 km) leads to a regressed radiative forcing of 2.8 ± 0.4 W m^{-2}. Black carbon added at higher layers in the lower and mid troposphere produces lower values of positive regressed radiative forcing; black carbon added near the tropopause (~12 km) and in the stratosphere causes negative regressed radiative forcing. Regressed radiative forcings are caused by increases in shortwave absorption from black carbon, changes in shortwave reflection from changes in clouds (especially low clouds), and changes in longwave radiation to space from changes in clouds (especially high clouds) and vertical profiles of temperature and water vapor. The aforementioned changes in temperature, clouds, and water vapor are those that occur on fast time-scales; they are associated with the fast tropospheric response from our black carbon additions, but not slow feedbacks that occur as global- and annual-average temperature changes and the climate system comes to equilibrium. Positive cloud forcing (Table 1) contributes to the positive regressed radiative forcing observed for additional near-surface (~0 km) black carbon. On the other hand, negative cloud forcing decreases the positive regressed radiative forcing for black carbon at ~1 and ~4 km. Large negative cloud forcing from black carbon near the tropopause (~12 km) contributes to the negative regressed radiative forcing in this simulation. For black carbon added to the stratosphere, cloud forcing is positive; negative regressed radiative forcing would be more negative if it were not for this positive cloud forcing. Note that these cloud changes are from thermodynamic changes in the atmosphere, the so-called semi-direct effect (Hansen et al. 1997; Johnson et al. 2004); indirect effects are not modeled in this study. Now we discuss changes in shortwave and longwave radiation separately.

3.1.1 Shortwave versus longwave regressed radiative forcing

The regressed radiative forcing comes from changes in both shortwave and longwave radiative fluxes, referred to here separately as regressed shortwave and longwave radiative forcing. All but one simulation has positive

Table 1 Regressed radiative forcing, fixed-SST radiative forcing, cloud forcing, fast response of cloud fractions, and equilibrium changes in surface air temperature and precipitation

Simulation (approximate altitude with additional black carbon)	0 km	1 km	4 km	12 km	20 km	29 km
Regressed radiative forcing and fast response of cloud variables[a]						
Regressed radiative forcing ($W\ m^{-2}$)[b, c]	2.78 ± 0.36[h]	0.50 ± 0.26	0.06 ± 0.18	−0.50 ± 0.29	−0.65 ± 0.40	−1.19 ± 0.33
Regressed shortwave radiative forcing ($W\ m^{-2}$)[c]	2.81 ± 0.42	0.98 ± 0.30	0.12 ± 0.17	−0.21 ± 0.29	4.69 ± 0.35	5.50 ± 0.40
Regressed longwave radiative forcing ($W\ m^{-2}$)[c]	−0.03 ± 0.19	−0.48 ± 0.19	−0.06 ± 0.12	−0.29 ± 0.15	−5.34 ± 0.25	−6.69 ± 0.19
Shortwave cloud forcing ($W\ m^{-2}$)[d]	1.52 ± 0.48	−0.16 ± 0.29	−1.27 ± 0.17	−2.14 ± 0.28	2.43 ± 0.40	3.20 ± 0.42
Longwave cloud forcing ($W\ m^{-2}$)[d]	−0.37 ± 0.18	0.01 ± 0.17	0.27 ± 0.09	−1.53 ± 0.12	−1.24 ± 0.22	−0.53 ± 0.18
Total cloud forcing ($W\ m^{-2}$)[d, e]	1.14 ± 0.40	−0.15 ± 0.25	−1.00 ± 0.17	−3.67 ± 0.28	1.18 ± 0.46	2.67 ± 0.35
Low cloud fraction	−0.015 ± 0.003	0.010 ± 0.002	0.030 ± 0.002	0.019 ± 0.002	0.000 ± 0.003	−0.007 ± 0.002
Medium cloud fraction	0.001 ± 0.002	−0.002 ± 0.002	−0.008 ± 0.001	0.012 ± 0.001	0.002 ± 0.002	0.002 ± 0.002
High cloud fraction	−0.004 ± 0.002	0.004 ± 0.002	0.008 ± 0.001	−0.018 ± 0.002	−0.014 ± 0.003	−0.006 ± 0.002
Total cloud fraction	−0.012 ± 0.003	0.009 ± 0.002	0.022 ± 0.002	0.002 ± 0.002	−0.006 ± 0.002	−0.007 ± 0.002
Fixed-SST radiative forcing[f]						
Fixed-SST radiative forcing ($W\ m^{-2}$)	1.79 ± 0.45	0.82 ± 0.45	0.51 ± 0.41	−0.72 ± 0.39	−0.82 ± 0.38	−1.62 ± 0.36
Fixed-SST shortwave radiative forcing ($W\ m^{-2}$)[c]	2.55 ± 0.41	1.41 ± 0.41	0.44 ± 0.34	−0.58 ± 0.32	4.35 ± 0.33	5.13 ± 0.31
Fixed-SST longwave radiative forcing ($W\ m^{-2}$)[c]	−0.77 ± 0.18	−0.59 ± 0.19	0.07 ± 0.23	−0.14 ± 0.22	−5.17 ± 0.17	−6.74 ± 0.18
Surface air temperature (K)	0.38 ± 0.12	0.11 ± 0.12	0.07 ± 0.12	−0.02 ± 0.12	−0.02 ± 0.12	−0.07 ± 0.12
Equilibrium climate response[g]						
Surface air temperature (K)	2.22 ± 0.07	0.62 ± 0.07	0.16 ± 0.07	−0.52 ± 0.07	−0.53 ± 0.07	−0.97 ± 0.07
Precipitation (% change)	4.10% ± 0.11%	−2.60% ± 0.11%	−3.71% ± 0.11%	−6.75% ± 0.11%	−3.73% ± 0.11%	−3.18% ± 0.11%

Values for regressed radiative forcing, cloud forcing, and fast response were calculated using the regression method of Gregory et al. (2004) by taking the *y*-intercept of regressions of the variables of interest versus changes in surface air temperature. Annual means of the first 20 years of three ensemble members were used in the regressions. Fixed-SST radiative forcing was calculated as the change in mean radiative imbalance (relative to the control) of simulations with fixed-SSTs

[a] All values are *y*-intercepts of regressions using the method of Gregory et al. (2004)

[b] Regressed radiative forcing is the sum of shortwave and longwave radiative forcing

[c] Fluxes are positive downward

[d] Positive cloud forcings indicate that changes in clouds cause increased energy to be absorbed by the climate system, and vice versa

[e] Sum of shortwave and longwave cloud forcing

[f] All values represent the mean of the last 35 years of 40-year simulations with prescribed climatological SSTs

[g] All values represent the mean of the last 70 years of 100-year simulations using a slab ocean

[h] Uncertainty estimate is given by 95% confidence interval

regressed shortwave radiative forcing (Table 1); note that the simulation with negative regressed shortwave radiative forcing (~12 km) is not statistically different from zero. All simulations have negative regressed longwave radiative forcing. The relative magnitude of shortwave versus longwave radiative forcing determines the sign of regressed radiative forcing. In general, positive regressed shortwave radiative forcing dominates for black carbon at low

altitudes, and negative longwave radiative forcing dominates for black carbon at high altitudes.

The addition of black carbon to the atmosphere causes changes in the shortwave radiation absorbed by the planet. The regressed shortwave radiative forcing comes both from the sunlight absorption of black carbon and changes in clouds (especially low clouds) that occur on fast timescales. These changes in clouds can occur from the heating surrounding black carbon, and at locations away from the black carbon due to changes in atmospheric stability, which will be later discussed. In some cases the changes in clouds can overwhelm the direct radiative effect of shortwave absorption from black carbon. For example, in the simulation that adds black carbon near the tropopause ($\sim$12 km), shortwave forcing is only -0.2 W m^{-2} because the negative shortwave cloud forcing is large enough to counter increases in shortwave absorption from black carbon (Table 1). The general trend in the troposphere is that as altitude increases, regressed shortwave radiative forcing decreases because of decreases in shortwave cloud forcing. This decrease in shortwave cloud forcing overwhelms the behavior that would cause increases in "instantaneous forcing" in the troposphere [i.e. that higher black carbon is less likely to be shaded by above clouds and more likely to intercept upward radiation that has been reflected by a lower altitude reflective cloud (e.g. Haywood and Shine 1997; Satheesh 2002; Hansen et al. 2005; Ming et al. 2005)]. The regressed shortwave radiative forcing is largest for black carbon added to the stratosphere. Positive shortwave cloud forcing contributes to over half of the regressed shortwave radiative forcing. Simulations with positive cloud forcing have corresponding fast response decreases in low cloud fraction, and vice versa (Table 1).

The addition of black carbon to the atmosphere causes increases in the longwave radiation escaping to space on fast timescales, and hence a negative regressed longwave radiative forcing, in all simulations. However, values for this forcing are small for black carbon added to the troposphere. Increases in outgoing longwave radiation are much larger for black carbon added to the stratosphere ($\sim$6 W m^{-2}). Changes in regressed longwave radiative forcing can come from increases in temperature surrounding black carbon (or more generally, changes in vertical temperature profiles), changes in the vertical profile of water vapor, and changes in clouds (especially high clouds). Again, these fast-response changes in clouds can come both from the heating surrounding black carbon and also at other layers due to changes in atmospheric stability, as will be further discussed in the next section. The fast response of longwave cloud forcing, presumably mostly due to the decrease in the high cloud fraction of 0.014 and changes in cloud droplet size (not reported), accounts for $\sim$23% of negative regressed radiative forcing from black carbon in the stratosphere at $\sim$20 km (Table 1). Simulations with positive longwave cloud forcing have corresponding increases in high cloud fraction, and vice versa (Table 1).

3.1.2 *Comparison with fixed-SST radiative forcing*

We re-ran the simulations with prescribed climatological SSTs to facilitate comparison of regressed radiative forcing and fixed-SST radiative forcing (Table 1). Mean values for radiative forcing appear quite different for these two methods. Note, however, that for the most part values are not statistically distinguishable. The exception is for the case of adding black carbon to the atmospheric surface layer, which gives radiative forcings of 2.78 ± 0.36 and 1.79 ± 0.45 W m^{-2} using the regression method and fixed-SST method, respectively. The difference stems from the fact that the regression method suggests a negligible longwave radiative forcing, whereas the fixed-SST method suggests a significant negative longwave radiative forcing.

3.2 Climate response

Whereas up until now we have discussed regressed and fixed-SST radiative forcing and fast responses of clouds, we now discuss the climate response from black carbon after the climate reaches equilibrium.

3.2.1 *Surface air temperature*

Changes in surface air temperature relative to the control for each model simulation are shown in Fig. 1 and Table 1 (also see Table S1 in Online Resource 2 for numerical values of other key climate variables). Addition of 1 Mt of black carbon near the surface increases surface air temperature by 2.22 ± 0.07 K. Black carbon added at higher layers in the lower and mid troposphere produces less surface warming; black carbon added near the tropopause ($\sim$12 km) and in the stratosphere decreases global mean surface air temperature by up to 0.97 ± 0.07 K. Surface temperature changes resulting from our horizontally uniform additions of black carbon are larger at the poles than at the equator (Fig. 2), in patterns that are similar to those observed for a doubling of atmospheric carbon dioxide (IPCC 2007). Polar surface temperatures are amplified by snow and sea ice feedbacks; equatorial surface temperatures are buffered by large surface latent heat fluxes.

3.2.2 *Climate feedback parameter and efficacy*

The trend in changes of surface air temperature versus the altitude of black carbon exhibits a high degree of correlation

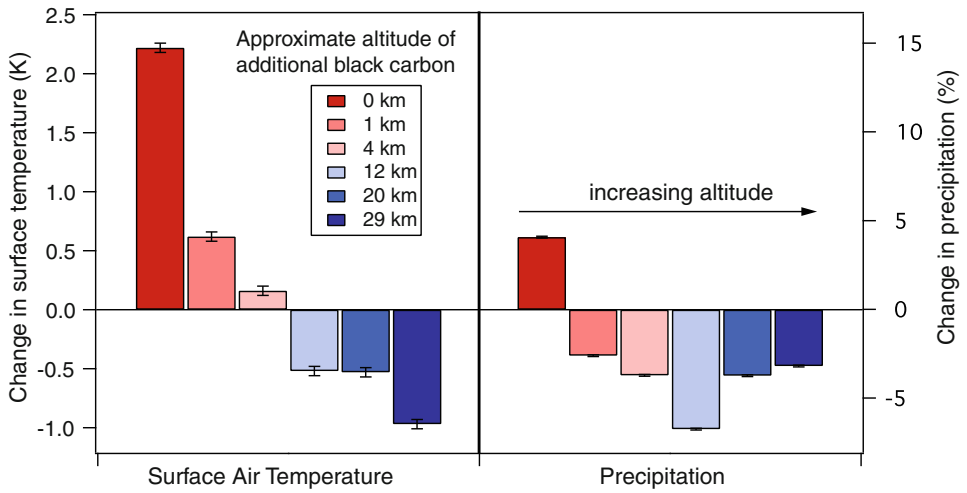

Fig. 1 Changes (relative to the control) for each simulation in global- and annual-mean surface air temperature and precipitation. In each simulation the concentration of black carbon is increased by 1 Mt at a different horizontal layer in the atmosphere. Approximate altitudes of layers with additional black carbon are indicated in the legend. Uncertainty is given by the standard error computed from 70 annual means using the Student *t* test with 95% confidence interval. The standard error is corrected for autocorrelation (Zwiers and von Storch 1995)

with regressed radiative forcing (Fig. 3). Simulations that show increases in surface air temperature (from low altitude black carbon) have associated positive regressed radiative forcing, and simulations showing decreases in surface temperature (from high altitude black carbon) have negative regressed radiative forcing. The equilibrium climate feedback parameter for our simulations, estimated as the slope of the best linear fits (constrained through the origin) of regressed radiative forcing versus equilibrium changes in surface air temperature (Ming et al. 2010), is 1.21 ± 0.16 W m^{-2} K^{-1} (uncertainty estimate is 95% confidence interval). This is indistinguishable from the feedback parameter for doubling CO_2 of 1.21 ± 0.41 W m^{-2} K^{-1} using the same method in this model (Bala et al. 2009). The efficacy for our black carbon simulations is calculated to be 1.00 ± 0.36 using values for regressed radiative forcing. Because the same feedback parameter was found for black carbon at various altitudes and for CO_2, this suggests that regressed radiative forcing, combined with an estimate of climate sensitivity to regressed radiative forcing changes, provides a consistent framework for predicting climate response to a climate forcing.

The basic trends seen with the regressed radiative forcing can also be observed for fixed-SST radiative forcing (Fig. 3). However, the climate feedback parameter, estimated as the slope of the best linear fits (constrained through the origin) of fixed-SST radiative forcing versus equilibrium changes in surface air temperature is 1.02 ± 0.45 W m^{-2} K^{-1}. This contrasts with the feedback parameter for doubling CO_2 of 1.61 ± 0.11 W m^{-2} K^{-1} using the same fixed-SST method in this model (Bala et al. 2009). The efficacy for our black carbon simulations is calculated to be 1.58 ± 0.70 using the values for fixed-SST forcing. Because the 95% confidence interval in the regression using fixed-SST radiative forcing (i.e. fixed-SST forcing versus equilibrium surface temperature change) is higher than that using regressed radiative forcing, and because the values of climate feedback parameter for black carbon and CO_2 are less consistent (i.e. the efficacy using the regression method is unity, whereas for the fixed-SST method it is 1.58), this suggests that fixed-SST radiative forcing may be a less reliable predictor of equilibrium temperature change. This is in agreement with Shine et al. (2003) who show in their Table 1 that fixed-SST forcing is a poor predictor of surface temperature change when varying the single scattering albedo of a globally uniform lower tropospheric aerosol layer. In contrast, Hansen et al. (2005) show that the efficacy of forcing in their simulations that increase black carbon in various horizontal layers is nearly unity when calculated using fixed-SST radiative forcing.

Climate feedback parameter and efficacy can also be calculated individually for each simulation (Table 2). Because of the relatively large uncertainties reported (95% CI), these results should be interpreted with caution. Efficacy values are near unity for the 0, 20, and 29 km simulations, calculated using the regression method of Gregory et al. Efficacy is larger than unity for the 1, 4, and 12 km simulations. Using the fixed-SST method for determining climate feedback parameter (Bala et al. 2009), values for efficacy are near unity for the 1, 12, and 20 km simulations. However, values for efficacy of black carbon at different altitudes (using both the regression and fixed-SST methods) are not statistically distinguishable, and thus we cannot conclude that efficacy values depend on the altitude

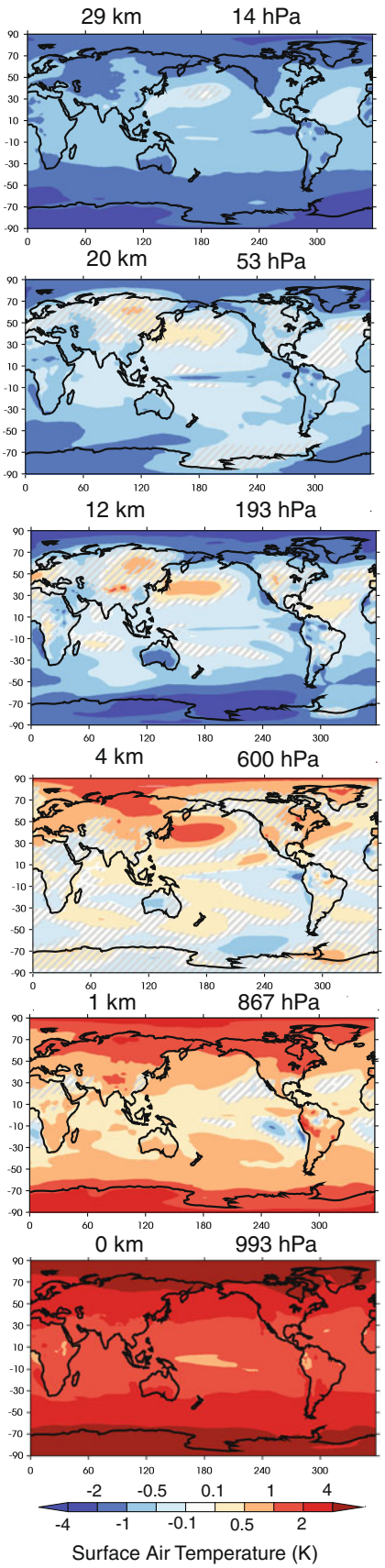

◀ **Fig. 2** Maps of changes in *surface* air temperature for each simulation (relative to the control). Each simulation increases black carbon aerosol concentrations by 1 Mt at a different horizontal layer in the atmosphere. The sigma hybrid pressure level and approximate corresponding altitude with additional black carbon is indicated above the figures. Hatches show areas where temperature changes do not significantly differ from zero at the 95% confidence level using the Student *t* test, based on the standard error computed from 70 annual means. The standard error is corrected for autocorrelation (Zwiers and von Storch 1995)

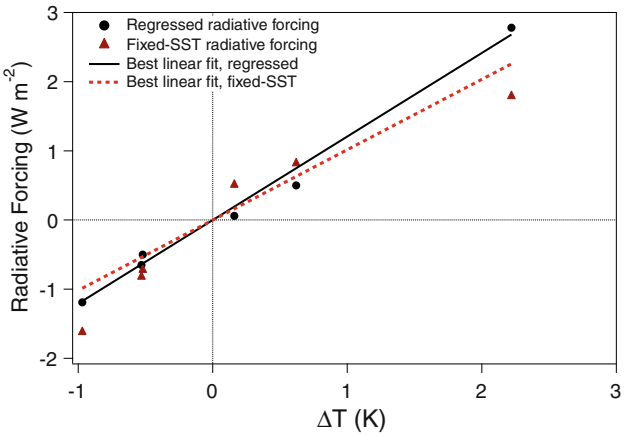

Fig. 3 Regressed radiative forcing and fixed-SST radiative forcing versus equilibrium changes in surface air temperature for each simulation. The slopes of each linear best fit (constrained through the origin), which can be interpreted as the climate feedback parameter for these simulations, are 1.21 ± 0.16 and 1.02 ± 0.45 W m^{-2} K^{-1}, using regressed and fixed-SST forcing, respectively. For reference, the feedback parameter for doubling CO_2 in this model is 1.21 ± 0.41 and 1.61 ± 0.11 W m^{-2} K^{-1} using regressed and fixed-SST radiative forcing (Bala et al. 2009). Efficacy of black carbon forcing in the simulations is calculated to be 1.00 ± 0.36 and 1.58 ± 0.70 using regressed radiative forcing and fixed-SST forcing, respectively. Uncertainty in all reported values is 95% confidence interval

of black carbon. Further, the proximity of the individual values to the regression line in Fig. 3 suggests that the feedback parameter (using regressed radiative forcing) is actually consistent among the simulations. Thus, the variation in climate response from black carbon at different altitudes occurs largely from different fast climate responses and not temperature dependent feedbacks.

3.2.3 *Vertical temperature profile*

Global mean vertical temperature profiles are shown in Fig. 4a. The largest temperature changes occur at the layers with additional black carbon due to diabatic heating, and consequently the simulation with additional black carbon near the surface (∼0 km) increases surface temperatures by the largest magnitude. As the altitude of additional black carbon increases, the surface temperature monoton-

Table 2 Climate feedback parameter and efficacy

Simulation (approximate altitude with additional black carbon)	Climate feedback parameter using regressed radiative forcing [(W m^{-2})/K][a]		Climate feedback parameter using fixed-SST forcing [(W m^{-2})/K][b]		Efficacy using regressed radiative forcing[c, d]		Efficacy using fixed-SST forcing[c, e]	
	Mean	Uncertainty (95% CI)	Mean	Uncertainty (95% CI)	Mean	Uncertainty (95% CI)	Mean	Uncertainty (95% CI)
0 km	1.25	0.17	0.98	0.26	0.96	0.35	1.65	0.44
1 km	0.81	0.43	1.60	0.98	1.50	0.95	1.01	0.61
4 km	0.39	1.17	5.74	9.89	3.13	9.56	0.28	0.48
12 km	0.96	0.57	1.41	0.86	1.27	0.86	1.14	0.69
20 km	1.23	0.78	1.61	0.86	0.99	0.71	1.00	0.53
29 km	1.22	0.36	1.78	0.48	0.99	0.44	0.90	0.24

Each metric is calculated two ways: (1) using regressed radiative forcing (Gregory et al. 2004)[a] and (2) using fixed-SST forcing and Eq. (5) from Bala et al. (2009)[b]. Results should be interpreted with caution because of the relatively high values of uncertainty (95% confidence interval). See Fig. 3 for an alternative method of calculating a "bulk" climate feedback parameter for the simulations

[a] Estimated as the regressed radiative forcing (Table 1) divided by the equilibrium surface air temperature change (Table 1)

[b] Estimated using Eq. (5) from Bala et al. (2009): $\Delta F_{\text{fixed-SST}}/(\Delta T_{\text{equilibrium}} - \Delta T_{\text{fixed-SST}})$, where $\Delta F_{\text{fixed-SST}}$ is the fixed-SST forcing (Table 1), and the ΔT terms are changes in surface air temperature from the simulations with slab ocean and fixed-SSTs (Table 1)

[c] Efficacy $\equiv$ Global temperature response per unit forcing for black carbon relative to that response to CO_2 forcing (Hansen et al. 2005)

[d] Climate sensitivity for CO_2 used in the calculation is 0.83 $\pm$ 0.28 K/(W m^{-2}), for a doubling of CO_2 (355–710 ppm) using the same model (Bala et al. 2009). Values of climate sensitivity parameter for black carbon and CO_2 use the regression method of Gregory et al. (2004) (see footnote (a), above)

[e] Climate sensitivity for CO_2 used in the calculation is 0.62 $\pm$ 0.04 K/(W m^{-2}), for a doubling of CO_2 (355–710 ppm) using the same model (Bala et al. 2009). Values of climate sensitivity parameter for black carbon and CO_2 use the fixed-SST method (see footnote (b), above)

ically decreases. This behavior was also observed in Hansen et al. (1997) when adding arbitrary heating source terms, which they call "ghost forcings," to various model layers. The ghost forcing created larger increases in surface temperature when at low altitudes than high altitudes. The simulated changes in vertical temperature profiles have implications on the stability of the atmosphere. For black carbon added in the surface layer, the vertical lapse rate is steepened and thus vertical stability is decreased; in contrast, black carbon higher in the atmosphere causes heating relative to the surface, making the lapse rate less steep, with corresponding increases in atmospheric stability. The stability changes affect convective transport and ultimately surface relative humidity, evaporation, and precipitation, as will be later discussed.

3.2.4 Vertical cloud profile

Equilibrium changes in the vertical distribution of cloud fraction caused by additional black carbon are shown in Fig. 4b. Localized heating from black carbon strongly decreases cloud cover in the layer in which it is added, as has been reported previously (Ackerman et al. 2000; Cook and Highwood 2004), and affects cloud cover in other layers (Fig. 4b). (Note that Ackerman et al. discuss specifically marine stratocumulus, while we discuss change in global-mean cloud amount.) Cloud cover reductions at the altitude of additional black carbon result from reductions in relative humidity associated with local heating (Hansen et al. 1997). Additional black carbon in the atmospheric surface layer ($\sim$0 km) decreases low clouds (Fig. 5a), which contributes to equilibrium surface warming. On the other hand, black carbon at $\sim$1 and $\sim$4 km increases low clouds, dampening surface warming; black carbon at $\sim$12 and $\sim$20 km also increases low clouds (Fig. 5a), but in these cases contribute to surface cooling.

Changes in global annual mean low clouds are primarily the result of fast response (i.e. the magnitude of the fast response is similar to that of the equilibrium response). For global annual mean high clouds, changes caused by aerosols high in the atmosphere are dominated by fast response, whereas changes caused by aerosols low in the atmosphere are dominated by slow response (see Figure S1 in Online Resource 1).

High clouds in our study are increased by black carbon from the surface layer to mid troposphere (Fig. 5a), contributing to surface warming, whereas high clouds are decreased by black carbon near the tropopause and in the stratosphere, contributing to surface cooling. The increase in high clouds from additional black carbon in the lower and mid-troposphere is inconsistent with results reported in Cook and Highwood (2004) for their simulations with interactive surface temperatures. (Cook and Highwood note that their results are mediated by surface temperature

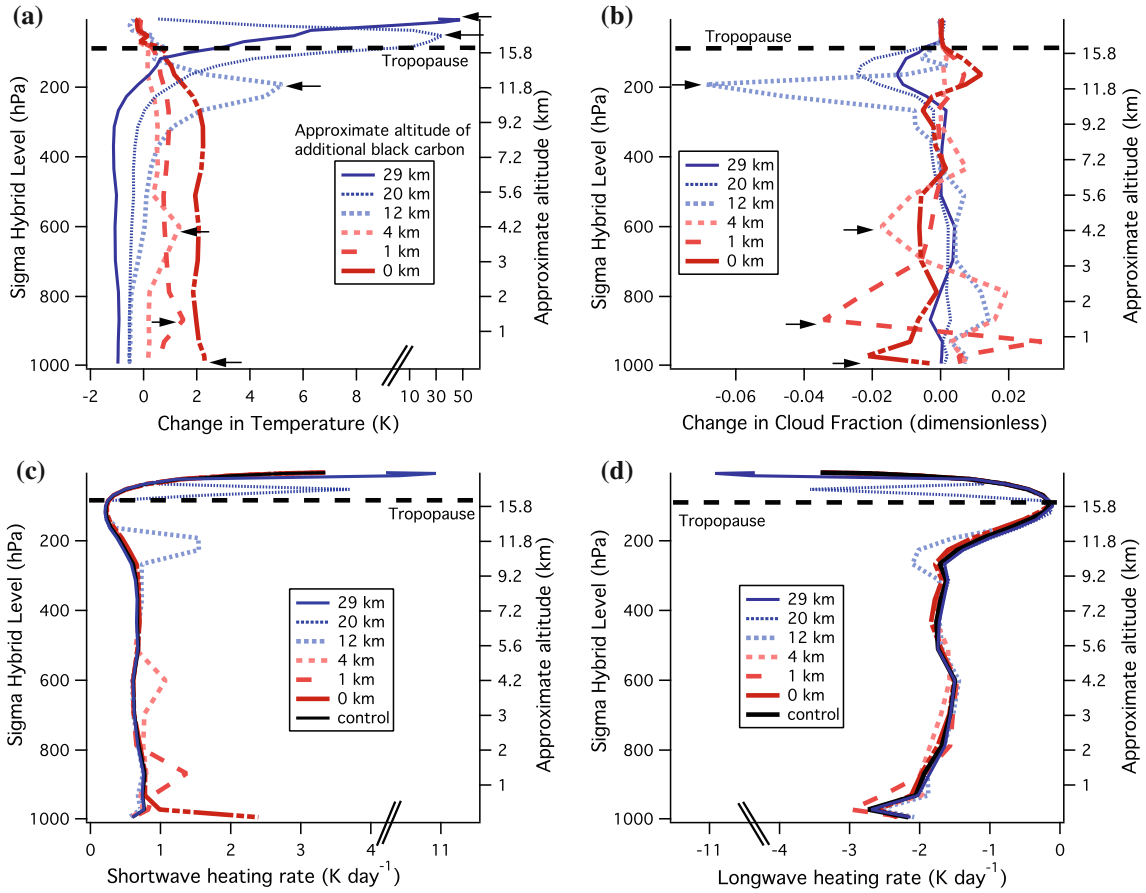

Fig. 4 Vertical profiles for changes (relative to the control) in **a** temperature, and **b** cloud fraction for each simulation. These profiles are calculated using area weighted global means for each model layer. Each simulation increases black carbon aerosol concentrations by 1 Mt at a different horizontal layer in the atmosphere. The black arrows show the layer with additional black carbon aerosol for each simulation. Note that temperatures increase and clouds decrease at the altitude with additional black carbon. *Panels* **c** and **d** show shortwave and longwave heating rates for each simulation; rather than showing changes relative to the control, **c** and **d** show actual values from each simulation (including the control)

and are therefore likely model dependent.) Note that inclusion of microphysical interactions between aerosols and clouds (i.e. indirect effects) in our study would likely alter the predicted effect of black carbon on the clouds in the layer where the black carbon concentrations are increased, which is further discussed in the Sect. 4.

3.2.5 Planetary energy budget

Addition of black carbon aerosols to the atmosphere changes the planetary energy budget of the equilibrium climate (Fig. 5b, c). Addition of black carbon aerosols at all altitudes reduces downward shortwave radiation reaching the surface (Fig. 5b), as has been previously reported (e.g. Ramanathan et al. 2001a; Ramanathan and Carmichael 2008). Even though a constant mass of black carbon is added to the atmosphere in each simulation, adding black carbon to different layers produces different changes in planetary albedo because of different cloud and snow/sea ice responses that alter surface albedo (Fig. 5c). Our simulations show that additional black carbon near the tropopause (~12 km) can lead to slight increases in planetary albedo due to the combination of increases in low clouds (Fig. 5a) and increased surface albedo (Fig. 5c) from increased snow and sea ice coverage.

Upward longwave radiation at the top of atmosphere increases in all but one simulation and balances changes in shortwave radiation as expected (Fig. 5b). Energy is more easily radiated to space from high altitudes than low altitudes (Hansen et al. 1997). This is important because black carbon aerosols absorb energy in the form of shortwave radiation and heat the surrounding atmosphere (Fig. 4c), causing changes in the vertical temperature profile and corresponding increases in longwave radiation at the altitude with additional black carbon (Fig. 4d). Approximately half of the increased longwave energy is emitted upward and half downward. The increase in upward longwave radiation is more efficiently lost to space when emitted at high altitudes

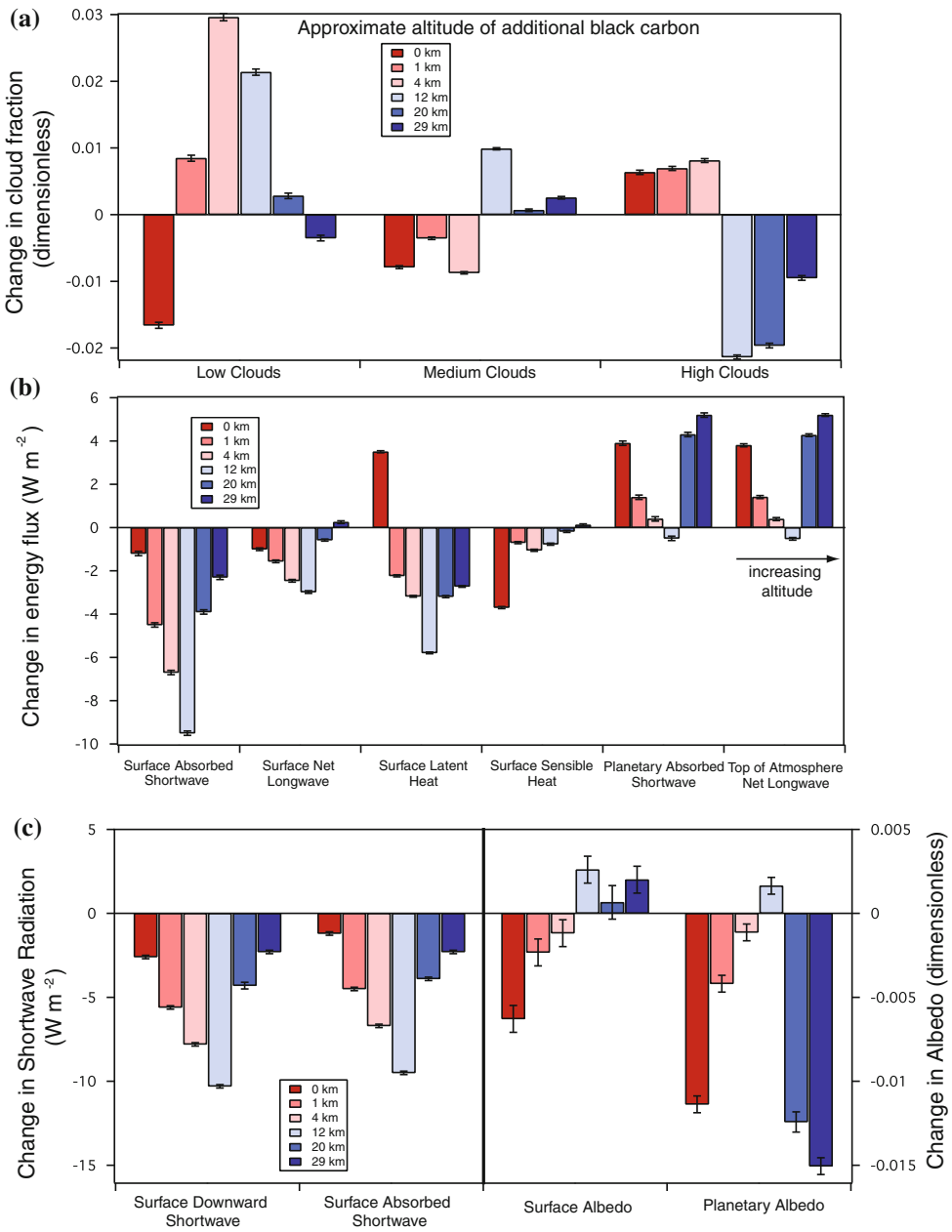

Fig. 5 Changes relative to the control for each simulation in **a** low, medium, and high clouds, **b** surface and top of atmosphere energy fluxes, and **c** surface downward and absorbed shortwave radiation, and surface and planetary albedo. Each simulation increases black carbon aerosol concentrations by 1 Mt at a different horizontal layer in the atmosphere. Approximate altitudes of layers with additional black carbon are indicated in the legend. Low clouds are those between the surface and ~3 km, medium clouds are between ~3 and ~7 km, and high clouds are above ~7 km. Longwave, sensible, and latent heat fluxes are positive upward; "surface absorbed shortwave" and "planetary absorbed shortwave" are equivalent to positive downward "surface net shortwave" and "top of atmosphere net shortwave," respectively. Uncertainty is given by the standard error computed from 70 annual means using the Student *t* test with 95% confidence interval. The standard error is corrected for autocorrelation (Zwiers and von Storch 1995)

(from black carbon at high altitudes) than from low altitudes (from black carbon at low altitudes), because longwave radiation emitted low in the atmosphere is likely to be absorbed by greenhouse gases. This behavior was observed previously in Hansen et al. (1997) when arbitrary heating source terms (called "ghost forcings") were added to different model layers; the energy was more efficiently lost to space when added at higher layers. The increased efficiency with which longwave radiation is lost to space at high altitudes contributes to the observed surface cooling from black carbon aerosols at high altitudes. This longwave effect is only evident in simulations that allow atmospheric temperatures to adjust to black carbon aerosols. Thus, instantaneous radiative forcing does not capture this effect.

3.2.6 *Precipitation: fast versus slow response*

Black carbon aerosols are thought to alter the hydrological cycle (e.g. Ramanathan et al. 2001a) largely because of changes in the surface energy budget. In our simulations, black carbon at all altitudes decreases the incident energy to the surface (Fig. 5c), which one might expect to reduce the amount of energy available to drive evaporation and thus lead to a decrease in precipitation. However, addition of black carbon to the atmospheric surface layer (~0 km) actually increases precipitation (Fig. 1). This likely occurs because black carbon in the surface layer heats the surface, steepening the vertical lapse rate and decreasing vertical stability; this leads to increased convective transport, lower

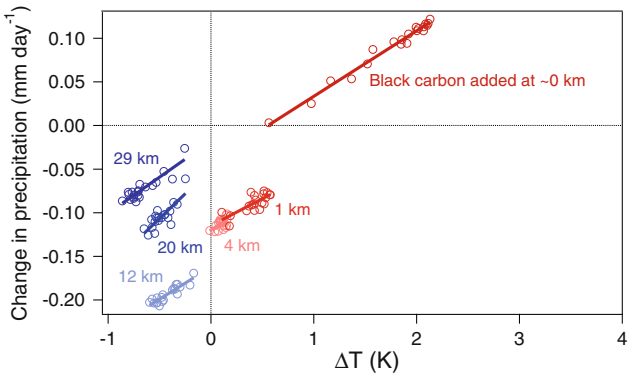

Fig. 6 Regressions of changes in precipitation versus changes in surface air temperature (relative to the control) following the method of Gregory et al. (2004). Annual means of the first 20 years of the simulations are used in the regressions. To decrease uncertainty, we ran a total of three 20-year simulations for each case of increased black carbon, and thus for each case the regressions are based on annual averages of the ensemble mean

relative humidity near the surface, increased evaporation (Fig. 5b), and thus increased precipitation.

Black carbon higher in the atmosphere increases atmospheric stability, contributing to decreases in precipitation (Fig. 1). For addition of black carbon at ~1 and ~4 km, the decreases in precipitation counters previous studies on greenhouse gases that have shown increases in precipitation with increases in surface air temperature at ~2 to 3% K^{-1} (Held and Soden 2006; Lambert and Webb 2008). Separating the fast and slow responses using the regression method of Gregory et al. (2004) provides further insight on the impact of black carbon on precipitation. As shown in Fig. 6, the slow response (interpreted as the slope of the regression) is 2.7% K^{-1}, which is consistent with the slow response from doubling of CO_2 of 2.8% ± 0.3 K^{-1} calculated using an ensemble of different slab-ocean GCMs (Andrews et al. 2009). Differences in equilibrium changes in precipitation stem from the varying fast responses (*y*-intercept of the regressions) from black carbon at different altitudes. In all simulations besides addition of black carbon in the lowest atmospheric layer and ~29 km, the equilibrium climate response is dominated by the fast response. It is worth noting again that aerosol indirect effects are not modeled in this study and are thus not contributing to changes in the hydrological cycle. Indirect effects are generally thought to decrease the efficiency with which precipitation is formed (Albrecht 1989).

4 Discussion

In this section we compare our results with those from other studies and discuss potential limitations of our study.

4.1 Comparison to other studies

Hansen et al. (2005) performed simulations using the GISS Model E global climate model in which black carbon was added to the lowest 8 model layers, where increases in black carbon are represented by increases in optical depth. Data presented in their Table 2 are shown graphically in our Figure S2 in Online Resource 3. The altitudes of the layers are not precisely known, but from Fig. 1 of Hansen et al. (2005), we estimate that the 8th layer is at an approximate altitude of 8 km (compared to our maximum altitude of ~29 km). As in our study, they do not model aerosol indirect effects. Results are qualitatively consistent with our results: as the altitude of black carbon increases in the troposphere, increases in surface temperature are smaller. Hansen et al. (2005) do not observe a change in sign of surface temperature response as we observe for black carbon near the tropopause and in the stratosphere (Fig. 1); this could be because they add black carbon to a maximum altitude on the order of 8 km. Like changes in surface temperature, regressed radiative forcing (which they refer to as Fs*, asymptotic planetary flux imbalance) also decreases as the altitude of additional black carbon increases, which is consistent with our results. Note that instantaneous and adjusted forcing increase with increasing altitude of black carbon in the troposphere, which is the opposite trend as that of surface temperature. This result is consistent with the fact that black carbon aerosols at high altitudes are more likely to be above reflective clouds, which has been reported elsewhere (e.g. Haywood et al. 1997; Haywood and Shine 1997; Satheesh 2002). The trend in instantaneous and adjusted forcing is not indicative of the trend in surface temperature for black carbon aerosols at different altitudes in the troposphere; therefore, in some cases it may be of secondary importance that black carbon aerosols at higher altitudes absorb more solar radiation than those at lower altitudes.

Penner et al. (2003) modeled the climate effects of emissions of soot consisting of both black carbon, which absorbs light, and a significantly larger fraction of organic mass, which scatters sunlight. The soot was emitted between 400 and 700 hPa. From their Fig. 1, it appears that the elevated emissions led to a maximum soot concentration increase at ~700 hPa (~3 km above the surface), but significant increases in aerosol concentrations exist from the surface to the stratosphere. From aerosol direct and semi-direct effects, they report an increase in temperature at altitudes surrounding their aerosol injections, which is consistent with our results. They find that temperatures decrease below ~800 hPa, though these temperature decreases are very small (<0.1 K), in part because they use fixed sea surface temperatures in their simulations. They find statistically insignificant fixed-SST radiative forcings

(which they refer to as "relaxed forcing"), due to the fact that their added aerosol both scatters and absorbs sunlight, and due to an increase in low stratiform clouds below 800 hPa. Similar to our results for additional high-altitude black carbon, they find a significant negative fixed-SST radiative forcing, which they attribute mostly to changes in the atmospheric vertical temperature profile and decreases in high clouds (near 500 hPa).

A recent paper (Ming et al. 2010) investigated the effects of absorbing aerosols on global-mean precipitation using the Geophysical Fluid Dynamics Laboratory (GFDL) AM2.1 atmosphere GCM coupled to a slab ocean model. They add globally uniform distributions of $\sim$1.2 Mt of black carbon to various layers in the atmosphere up to an altitude of $\sim$4 km. Their results do not show a coherent trend for changes in surface air temperature versus the altitude of additional black carbon. Note however that Ming et al. represent aerosol indirect effects (though for aerosols other than black carbon and dust) and thus our results are not directly comparable. As in our study, they find that black carbon at low altitudes (between the surface and $\sim$0.8 km) can increase precipitation, whereas higher altitude black carbon (between $\sim$1.4 km and their highest altitude black carbon addition of $\sim$4 km) can decrease precipitation.

4.2 Limitations of our study

As has already been discussed, our simulations include aerosol direct effects and semi-direct effects. Since the model used in this study is simpler than reality, our results are somewhat dependent on the accuracy with which the atmosphere of the model responds to heating from black carbon. A previous study comparing simulations with a large eddy model (where turbulence and cloud dynamics are explicitly resolved) versus a single column version of a GCM (NCAR Single-Column Community Climate Model) found that aerosol radiative forcing from the semi-direct effect was five times smaller in the single column model than the large eddy model (Johnson 2005). This occurred because cloud responses were underestimated by the parameterizations of cloud cover and cloud radiative properties in the single column model. Similar studies using single column versions of more modern GCMs with better model physics are desired.

The present study does not model aerosol indirect effects in which particles act as cloud condensation nuclei. These cloud condensation nuclei would be expected to increase cloud albedo and cloud lifetime (Twomey 1977; Albrecht 1989). Black carbon can have additional effects on cloud microphysics by heating its immediate surroundings (Nenes et al. 2002). Including aerosol indirect effects in a study of this type is an important topic for future study. Given the uncertain nature of aerosol indirect effects, it is not immediately clear how their inclusion in this study would alter our results. In Penner et al. (2003), including aerosol indirect effects decreased the fixed-SST shortwave radiative forcing (which they refer to as shortwave relaxed forcing) to a statistically significant negative value (as opposed to the insignificant positive value without including indirect effects), but longwave forcing remained approximately the same. Note that wet deposition is the primary removal mechanism of atmospheric aerosols. Thus, through indirect effects aerosols have the potential to alter their own removal mechanisms.

In our study we analyze the sensitivity of radiative forcing and climate response relative to a modern background aerosol distribution. Note that the quantitative results may be somewhat dependent on the background aerosol distribution used. Also, relative differences in shortwave heating rates (Fig. 4c) occur in part because of the fact that sigma hybrid layers at higher altitudes are shallower in terms of mass. The relatively larger heating rates that occur from black carbon in the stratosphere could potentially affect the magnitude of the semi-direct effect (i.e. the magnitude of the decreases in high clouds in the simulations with additional black carbon in the stratosphere could be reduced with lower stratospheric heating rates). Nonetheless, the qualitative results should be unchanged.

5 Conclusions

Black carbon aerosols absorb solar radiation in the atmosphere and thus reduce downward solar radiation at the surface of Earth. However, as shown by our highly idealized climate simulations, black carbon at low altitudes warms the surface through direct diabatic heating. In contrast, black carbon at high altitudes increases the amount of solar radiation absorbed at high altitudes, but this absorbed energy is largely lost to space in the form of increased longwave radiation without heating the lower troposphere. In addition, high altitude black carbon reduces high altitude cloud cover. Thus, despite increasing planetary absorption of shortwave radiation (i.e. reducing planetary albedo), high-altitude black carbon aerosols can produce surface cooling.

Black carbon aerosols tend to heat the layer they are in. This heating not only "burns off" clouds in this layer, but also alters clouds in other layers by impacting the vertical temperature profile and thus atmospheric stability. Black carbon added to the lowest atmospheric layer decreases vertical stability and increases convection, drying the surface layer and increasing evaporation and thus precipitation. This increase in surface latent heat flux (Fig. 5b) and precipitation (Fig. 1) occurs despite a reduction in solar

radiation reaching the surface. For black carbon at higher altitudes in the troposphere, heating from black carbon stabilizes the atmosphere below the heated layer, diminishing convection, moistening the surface layer, and decreasing evaporation and thus precipitation. Black carbon in the mid troposphere decreases surface evaporation (Fig. 5b) despite surface warming. Variations in equilibrium climate response of precipitation (and thus evaporation) for black carbon at different altitudes largely stem from variations in the fast climate response (Fig. 6). The slow climate response for precipitation was 2.7% K^{-1} from black carbon at different altitudes, which is consistent with the slow response from doubling of CO_2 of 2.8% K^{-1} calculated using an ensemble of different slab-ocean GCMs (Andrews et al. 2009).

Our results suggest that regressed radiative forcing (Gregory et al. 2004) is a better predictor of equilibrium changes in surface air temperature than is fixed-SST forcing. This general result agrees with Shine et al. (2003) but somewhat disagrees with the results of Hansen et al. (2005), though in both of these studies fixed-SST forcing is a better predictor of temperature change from aerosols than is instantaneous and adjusted forcing. The equilibrium climate feedback parameter for our simulations calculated using regressed radiative forcing is 1.21 ± 0.16 W m^{-2} K^{-1} (uncertainty estimate is 95% confidence interval). This is indistinguishable from the feedback parameter for doubling CO_2 of 1.21 ± 0.41 W m^{-2} K^{-1} in this model, also calculated using regressed radiative forcing (Bala et al. 2009). The climate feedback parameter for our simulations calculated using the fixed-SST forcing is 1.02 ± 0.45 W m^{-2} K^{-1}. This contrasts with the feedback parameter for doubling CO_2 of 1.61 ± 0.11 W m^{-2} K^{-1} in this model, calculated using fixed-SST forcing (Bala et al. 2009). The variation in climate response from black carbon at different altitudes occurs largely from different fast climate responses and not temperature dependent feedbacks.

The importance of the altitude of absorbing aerosols in determining their climate response points to the value of properly measuring and modeling aerosol vertical profiles in the atmosphere. Measurements of this type are needed at the global scale. In addition, models that include aerosol transport need to accurately represent convective lofting for accurate portrayal of the effects of aerosols on climate (Penner et al. 2003).

References

Ackerman AS, Toon OB, Stevens DE, Heymsfield AJ, Ramanathan V, Welton EJ (2000) Reduction of tropical cloudiness by soot. Science 288:1042–1047

Albrecht BA (1989) Aerosols, cloud microphysics, and fractional cloudiness. Science 245:1227–1230

Andrews T, Forster PM, Gregory JM (2009) A surface energy perspective on climate change. J Clim 22:2557–2570

Bala G, Caldeira K, Nemani R (2009) Fast versus slow response in climate change: implications for the global hydrological cycle. Clim Dyn. doi:10.1007/s00382-00009-00583-y

Bond TC, Streets DG, Yarber KF, Nelson SM, Woo JH, Klimont Z (2004) A technology-based global inventory of black and organic carbon emissions from combustion. J Geophys Res Atmos 109. doi:10.1029/2003JD003697

Cess RD (1985) Nuclear-war—illustrative effects of atmospheric smoke and dust upon solar-radiation. Clim Change 7:237–251

Collins WD, Rasch PJ, Eaton BE, Khattatov BV, Lamarque JF, Zender CS (2001) Simulating aerosols using a chemical transport model with assimilation of satellite aerosol retrievals: methodology for INDOEX. J Geophys Res Atmos 106:7313–7336

Collins WD, Rasch PJ, Eaton BE, Fillmore DW, Kiehl JT, Beck CT, Zender CS (2002) Simulation of aerosol distributions and radiative forcing for INDOEX: regional climate impacts. J Geophys Res Atmos 107. doi:10.1029/2000JD000032

Collins WD et al (2004) Description of the NCAR community atmosphere model (CAM 3.0). NCAR technical note NCAR/TN-464+STR. National Center for Atmospheric Research, Boulder, CO

Cook J, Highwood EJ (2004) Climate response to tropospheric absorbing aerosols in an intermediate general-circulation model. Q J R Meteorol Soc 130:175–191

Covey C, Schneider SH, Thompson SL (1984) Global atmospheric effects of massive smoke injections from a nuclear-war—results from general-circulation model simulations. Nature 308:21–25

Gregory JM, Ingram WJ, Palmer MA, Jones GS, Stott PA, Thorpe RB, Lowe JA, Johns TC, Williams KD (2004) A new method for diagnosing radiative forcing and climate sensitivity. Geophys Res Lett 31. doi:10.1029/2003GL018747

Hansen J, Sato M, Ruedy R (1997) Radiative forcing and climate response. J Geophys Res Atmos 102:6831–6864

Hansen J et al. (2005) Efficacy of climate forcings. J Geophys Res Atmos 110. doi:10.1029/2005JD005776

Haywood JM, Ramaswamy V (1998) Global sensitivity studies of the direct radiative forcing due to anthropogenic sulfate and black carbon aerosols. J Geophys Res Atmos 103:6043–6058

Haywood JM, Shine KP (1997) Multi-spectral calculations of the direct radiative forcing of tropospheric sulphate and soot aerosols using a column model. Q J R Meteorol Soc 123:1907–1930

Haywood JM, Roberts DL, Slingo A, Edwards JM, Shine KP (1997) General circulation model calculations of the direct radiative forcing by anthropogenic sulfate and fossil-fuel soot aerosol. J Climate 10:1562–1577

Haywood JM, Donner LJ, Jones A, Golaz J-C (2009) Gobal indirect radiative forcing caused by aerosols: IPCC (2007) and beyond. In: Heintzenberg J, Charlson R (eds) Clouds in the perturbed climate system. MIT Press, Cambridge, pp 451–467

Held IM, Soden BJ (2006) Robust responses of the hydrological cycle to global warming. J Clim 19(21):5686–5699. doi:10.1175/JCLI3990.1

Hess M, Koepke P, Schult I (1998) Optical properties of aerosols and clouds: the software package OPAC. Bull Am Meteorol Soc 79:831–844

IPCC (1990) Climate change: the IPCC scientific assessment. Contribution of Working Group 1 to the first assessment report of the Intergovernmental Panel on Climate Change. Cambridge University Press, Cambridge

IPCC (2007) Climate change 2007: the physical science basis. Contribution of Working Group 1 to the fourth assessment report of the Intergovernmental Panel on Climate Change. In: Solomon S, Qin D, Manning M, Chen Z, Marquis M, Averyt KB, Tignor M, Miller HL (eds). Cambridge University Press

Johnson BT (2005) The semidirect aerosol effect: comparison of a single-column model with large eddy simulation for marine stratocumulus. J Climate 18:119–130

Johnson BT, Shine KP, Forster PM (2004) The semi-direct aerosol effect: impact of absorbing aerosols on marine stratocumulus. Q J R Meteorol Soc 130:1407–1422

Kalnay E et al (1996) The NCEP/NCAR 40-year reanalysis project. B Am Meteorol Soc 77:437–471

Lambert FH, Webb MJ (2008) Dependency of global mean precipitation on surface temperature. Geophys Res Lett 35:L16706

Lohmann U, Rotstayn L, Storelvmo T, Jones A, Menon S, Quaas J, Ekman AML, Koch D, Ruedy R (2010) Total aerosol effect: radiative forcing or radiative flux perturbation? Atmos Chem Phys 10:3235–3246

Ming Y, Ramaswamy V, Ginoux PA, Horowitz LH (2005) Direct radiative forcing of anthropogenic organic aerosol. J Geophys Res Atmos 110. doi:10.1029/2004jd005573

Ming Y, Ramaswamy V, Persad G (2010) Two opposing effects of absorbing aerosols on global-mean precipitation. Geophys Res Lett 37. doi:10.1029/2010GL042895

Nenes A, Conant WC, Seinfeld JH (2002) Black carbon radiative heating effects on cloud microphysics and implications for the aerosol indirect effect—2. Cloud microphysics. J Geophys Res Atmos 107. doi:10.1029/2002jd002101

Oleson KW et al (2004) Technical description of the community land model (CLM). NCAR technical note NCAR/TN-461+STR. National Center for Atmospheric Research, Boulder, CO

Penner JE, Zhang SY, Chuang CC (2003) Soot and smoke aerosol may not warm climate. J Geophys Res Atmos 108. doi:10.1029/2003JD003409

Ramanathan V, Carmichael G (2008) Global and regional climate changes due to black carbon. Nature Geosci 1:221–227

Ramanathan V, Crutzen PJ, Kiehl JT, Rosenfeld D (2001a) Atmosphere—aerosols, climate, and the hydrological cycle. Science 294:2119–2124

Ramanathan V et al (2001b) Indian Ocean experiment: an integrated analysis of the climate forcing and effects of the great Indo-Asian haze. J Geophys Res Atmos 106:28371–28398

Ramaswamy V, Kiehl JT (1985) Sensitivities of the radiative forcing due to large loadings of smoke and dust aerosols. J Geophys Res Atmos 90:5597–5613

Rasch PJ, Mahowald NM, Eaton BE (1997) Representations of transport, convection, and the hydrologic cycle in chemical transport models: implications for the modeling of short-lived and soluble species. J Geophys Res Atmos 102:28127–28138

Satheesh S (2002) Aerosol radiative forcing over land: effect of surface and cloud reflection. Ann Geophys 20:2105–2109

Seinfeld J (2008) Atmospheric science—black carbon and brown clouds. Nature Geosci 1:15–16

Seinfeld JH, Pandis SN (1998) Atmospheric chemistry and physics: from air pollution to climate change. Wiley-Interscience Publication, Hoboken

Shine KP, Cook J, Highwood EJ, Joshi MM (2003) An alternative to radiative forcing for estimating the relative importance of climate change mechanisms. Geophys Res Lett 30:1–4

Stowe LL, Ignatov AM, Singh RR (1997) Development, validation, and potential enhancements to the second-generation operational aerosol product at the National Environmental Satellite, Data, and Information Service of the National Oceanic and Atmospheric Administration. J Geophys Res Atmos 102:16923–16934

Turco RP, Toon OB, Ackerman TP, Pollack JB, Sagan C (1983) Nuclear winter—global consequences of multiple nuclear-explosions. Science 222:1283–1292

Twomey S (1977) Influence of pollution on shortwave albedo of clouds. J Atmos Sci 34:1149–1152

Zwiers FW, von Storch H (1995) Taking serial-correlation into account in tests of the mean. J Climate 8:336–351